

N₂O Adsorption and Photochemistry on High Area TiO₂ Powder

C. N. Rusu and J. T. Yates, Jr.*

Surface Science Center, Department of Chemistry, University of Pittsburgh, Pittsburgh, Pennsylvania 15260

Received: October 31, 2000

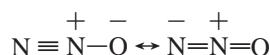
The adsorption and photochemistry of N₂O chemisorbed on TiO₂ powder has been investigated. At 157 K, nitrous oxide is molecularly adsorbed on the reduced titanium dioxide. Adsorption on the TiO₂ surface takes place through both the N and O ends of the nitrous oxide molecule. The photochemistry of the adsorbed N₂O molecules was studied at 157 K by use of UV irradiation in the range 2.1–5.0 eV. The photoactivity of the adsorbed molecule is dependent on the N₂O coverage. At low coverages, the adsorbed N₂O is photodepleted to produce adsorbed nitrogen. Larger coverages of N₂O are not photodepleted to N₂ due to the site blocking in the adsorption process. N-bonded species show a higher photoreactivity than the O-bonded species. Photoformation of NO was not observed at any N₂O coverage.

I. Introduction

Nitrous oxide (N₂O), although present in relatively low concentrations, is an air pollutant because of its contribution to ozone depletion through photochemical reactions in the stratosphere. Atmospheric N₂O also contributes to global warming through its high greenhouse efficiency. N₂O emissions in the atmosphere derive from both natural and anthropogenic sources. Primary anthropogenic sources of N₂O emissions are cultivated soils, biomass burning, and chemical production. N₂O is also present, although in small quantities, in combustion exhaust gases. Therefore, finding a photochemical method to decompose N₂O is very desirable. An overview of the heterogeneous thermally induced catalytic decomposition of N₂O over metals, pure and mixed oxides, and zeolitic systems was written by Kapteijn et al.¹

Nitrous oxide adsorption has been studied on many different types of surfaces including alkali halides,² metal oxides,^{3–7} and metals.^{8,9} The adsorption of nitrous oxide on semiconductors,^{6,7,10–12} in particular on TiO₂,^{7,11} was shown to cause the decomposition of the N₂O molecule. Shultz et al.,¹¹ using X-ray photoelectron spectroscopy (XPS) and SHG, proved that N₂O heals the defects present on the TiO₂(110) defective surface by dissociation so that no nitrogen remains on the surface and the oxygen atoms are incorporated into the lattice.

Two resonance structures can be drawn for the N₂O molecule:



For N₂O adsorption on the oxide surfaces, there is evidence for both N- and O-bonded adsorption complexes. The evidence for these two adsorbate structures, which differ in their bonding configuration, has been primarily proved through analysis of the vibrational data. An early study by Zecchina et al.¹³ of nitrous oxide adsorption on α -Cr₂O₃ showed the presence of both N- and O-bonded N₂O-adsorbed surface species, both moieties being bonded to the Cr³⁺ sites. Figure 1 shows the frequencies observed for N₂O adsorbed on TiO₂ as well as on several other oxide surfaces such as ZrO₂,⁵ α -Cr₂O₃,^{13,14} and Al₂O₃,⁴ in comparison with the vibrational modes for N₂O gas¹⁵ and N₂O in solid phase.¹⁶ The asymmetric stretch, situated in

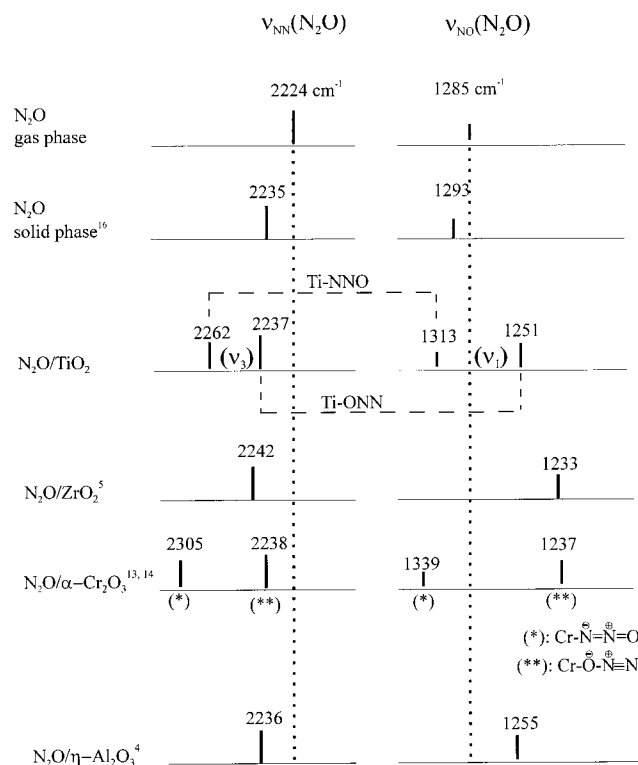


Figure 1. Vibrational modes of the N₂O molecule adsorbed on different substrates in comparison with N₂O in the gas and solid phases. The asymmetric stretch, situated in the range 2200–2300 cm⁻¹, can be described as a nitrogen–nitrogen stretching motion. The symmetric stretch, situated in the 1200–1350 cm⁻¹ range, can be described as a nitrogen–oxygen stretching motion.

the range 2200–2300 cm⁻¹, can be described as a nitrogen–nitrogen stretching motion. The symmetric stretch, situated in the 1200–1350 cm⁻¹ range, can be described as a nitrogen–oxygen stretching motion.^{13,14}

Photocatalytic decomposition of N₂O over ZnO was studied in the temperature range 644–704 K by Tanaka and Blyholder.¹⁷ At these temperatures, both thermal and photocatalytic decomposition occur. The kinetics of these processes were determined. Cunningham et al. have reported that the decomposition of N₂O

is photoinduced over ZnO through the trapping of photogenerated electrons from the ZnO substrate by N₂O molecules.^{18,19} UV irradiation of nitrous oxide in the presence of titanium oxide anchored onto porous Vycor glass was studied by Anpo et al.^{20,21} Nitrogen is formed in the N₂O photodecomposition process at 300 K. On the other hand, on the basis of electron paramagnetic resonance (EPR) studies and by use of isotopically labeled compounds, it was found by the same group that UV irradiation of the anchored titanium dioxide in the presence of N₂O at 77 K led to the formation of an unstable anion radical, N₂O⁻. The EPR signal arising from N₂O⁻ decreased when the temperature increased from 77 to 298 K and practically disappeared at 298 K. Simultaneously, the evolution of nitrogen was found to take place during these experiments. On the basis of their studies, the authors concluded that the photocatalytic decomposition of N₂O on the anchored titanium dioxide proceeds through electron scavenging by N₂O with the formation of N₂O⁻ followed by its decomposition to nitrogen and O⁻.²² Ag- and Cu-supported catalysts on TiO₂ showed higher photoactivity in comparison with other supports used (ZnO, PbO, WO₃, SrTiO₃, etc.) for the reduction of N₂O to N₂ at room temperature, in the presence of methanol and water vapors, but no comparison with pure TiO₂ was done.¹⁰

The work presented in this paper involves studies of N₂O adsorption and photodecomposition on reduced TiO₂ powder. The purpose of these studies was not only to find out if TiO₂ is a good photocatalyst for the N₂O decomposition but also to check whether NO is one of the products of the N₂O photodecomposition. This information was desired for correlation with one of our previous papers.²³ We showed there²³ that the NO photochemistry on TiO₂(110) at 118 K leads mainly to the formation of photodesorbed N₂O. We postulated that it is possible that the simultaneous formation of minor quantities of NO may originate from the partial photodecomposition of N₂O.

Our present studies show that NO is not produced in the photodecomposition of N₂O adsorbed on TiO₂ powder.

II. Experimental Section

Experiments were carried out in a bakeable stainless steel IR cell capable of operating at sample temperatures from 100 to 1500 K. A detailed description of the IR cell had been reported previously.²⁴ In brief, the TiO₂ powder was pressed into a tungsten grid, which was held rigidly by a power/thermocouple feedthrough via a pair of nickel clamps. A K-type thermocouple was spot-welded on the top-central region of the tungsten grid to measure the temperature of the sample. The sample temperature could be easily adjusted by use of liquid nitrogen and electrical heating of the grid via a programmable controller.²⁵ The TiO₂ sample was pressed only on half of the tungsten grid, while the other half of the grid had no sample. The infrared spectra of the TiO₂ surface and of the gaseous species could be measured alternatively by translating the cell in the spectrometer, between the two half-sections of the grid.

The IR cell was connected to a stainless steel vacuum system pumped by both turbomolecular and ion pumps and the base pressure was lower than 1×10^{-8} Torr. The system base pressure was measured by the ion current drawn by the ion pump (Varian, 921-0062), while reactant gas pressures were measured by a capacitance manometer (Baratron, 116A, MKS, range 10^{-3} – 10^3 Torr). A Fourier transform infrared (FTIR) spectrometer and a quadrupole mass spectrometer (Dycor Electronics Inc.) were used in this system. The sample cell is mounted on a computer-controlled precision 2D-translation system ($\pm 1 \mu\text{m}$ accuracy) made with components from the Newport Corpora-

tion. This system allows the cell to move reproducibly inside the spectrometer cavity as the sample or the gas phase are being measured.

Infrared spectra were obtained with a nitrogen gas-purged Mattson Fourier transform infrared spectrometer (Research Series 1) equipped with a wide-band HgCdTe detector. The sample spectra shown here were recorded with 4 cm^{-1} resolution for 1000 scans, while the background spectra were recorded with 4 cm^{-1} resolution for 2000 scans.

The TiO₂ used was Degussa titanium dioxide P25, which is reported to have 70% anatase and 30% rutile composition and a surface area of $\sim 50 \text{ m}^2/\text{g}$ at room temperature.^{26,27}

The UV source is a 350 W high-pressure mercury arc lamp (Oriol Corp.). The power received by the sample measured for the full Hg arc (2.1–5 eV) was $660 \text{ mW}/\text{cm}^2$. A manual shutter was installed to accurately control the UV exposure time. The TiO₂ sample on the tungsten grid was positioned in such a way that both the IR beam from the FTIR spectrometer and the UV light from the mercury arc are focused on it at an angle of incidence of about 45° to the normal of the grid.²⁸ The orthogonal arrangement of UV light with the IR beam makes IR measurements possible during photochemistry on the surface.

The N₂O (99.999% purity) was obtained from Matheson Gas Products and was purified by freeze–pump–thaw cycles.

The N₂O adsorption and photodepletion experiments were carried out on powdered TiO₂ treated as follows: after oxidation of the TiO₂ at 673 K in O₂(g) at 6 Torr for 30 min, the sample was heated in a vacuum to 900 K for 1 h and then for 13 h, in vacuum, at 800 K in order to activate the surface. N₂O was then adsorbed at 157 K. During the UV irradiation, the course of the photodepletion reaction was continuously monitored by FTIR measurements.

III. Results

1. N₂O Adsorption on TiO₂. Figure 1 shows a summary of the vibrational frequencies for N₂O that form a basis for this paper. It is noted that for N₂O adsorbed on TiO₂, ν_3 corresponding to the N–N stretching mode is broken into two bands and that also ν_1 (N–O stretching mode) consists of two components. This is undoubtedly due to the two structures of chemisorbed N₂O on TiO₂: N-bonded and O-bonded.

The most intense infrared absorptions of N₂O adsorbed on TiO₂ at 157 K are reported in Figure 2. For increasing N₂O coverages, two most intense groups of bands were observed: one group in the 2300 – 2200 cm^{-1} range with a larger absorbance and another group in the 1350 – 1200 cm^{-1} range with a smaller absorbance. Although the frequencies of the bands are shifted from the N₂O(g) values of 2224 and 1285 cm^{-1} ,¹⁵ these modes are identified respectively as the asymmetric stretch, ν_3 (NN stretch), and the symmetric stretch, ν_1 (NO stretch), of adsorbed N₂O on TiO₂. The 2262 and 2237 cm^{-1} bands are both blue-shifted comparing with the NN stretch frequency of 2224 cm^{-1} for N₂O in the gas phase. In contrast, for the ν_1 (NO stretch) mode, the 1251 cm^{-1} vibrational mode is red-shifted compared to the N₂O(g) mode at 1285 cm^{-1} . However, the 1313 cm^{-1} vibrational mode is blue-shifted comparing with the N₂O(g). Weak absorption bands (not shown) are seen at 3456 cm^{-1} , corresponding to the combination ($\nu_1 + \nu_3$) absorption band, and at 2499 cm^{-1} , corresponding to the overtone ($2\nu_1$).

Figure 3 (upper panel) shows the evolution of the absorbance of the main absorption bands at 2237 , 2262 , 1251 , and 1313 cm^{-1} as the N₂O exposure to the TiO₂ sample increased. To observe the correlation between these absorption bands, their

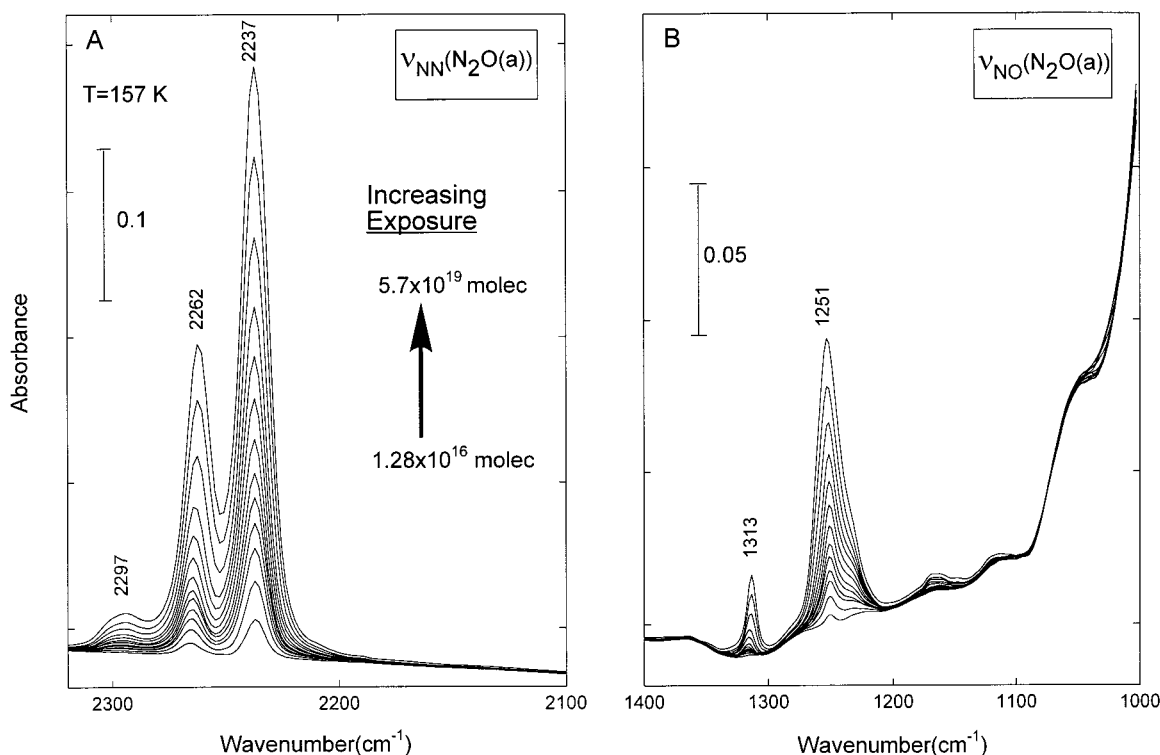


Figure 2. IR spectra of adsorbed N_2O molecules on TiO_2 powder as a function of N_2O exposure at 157 K. The N_2O exposure increases from 1.28×10^{16} N_2O molecules added, which corresponds to the first (bottom) spectrum, to 5.70×10^{19} N_2O molecules added, which corresponds to the last (top) spectrum. The left panel corresponds to the nitrogen–nitrogen stretching vibration, and the right panel corresponds to the nitrogen–oxygen stretching vibration.

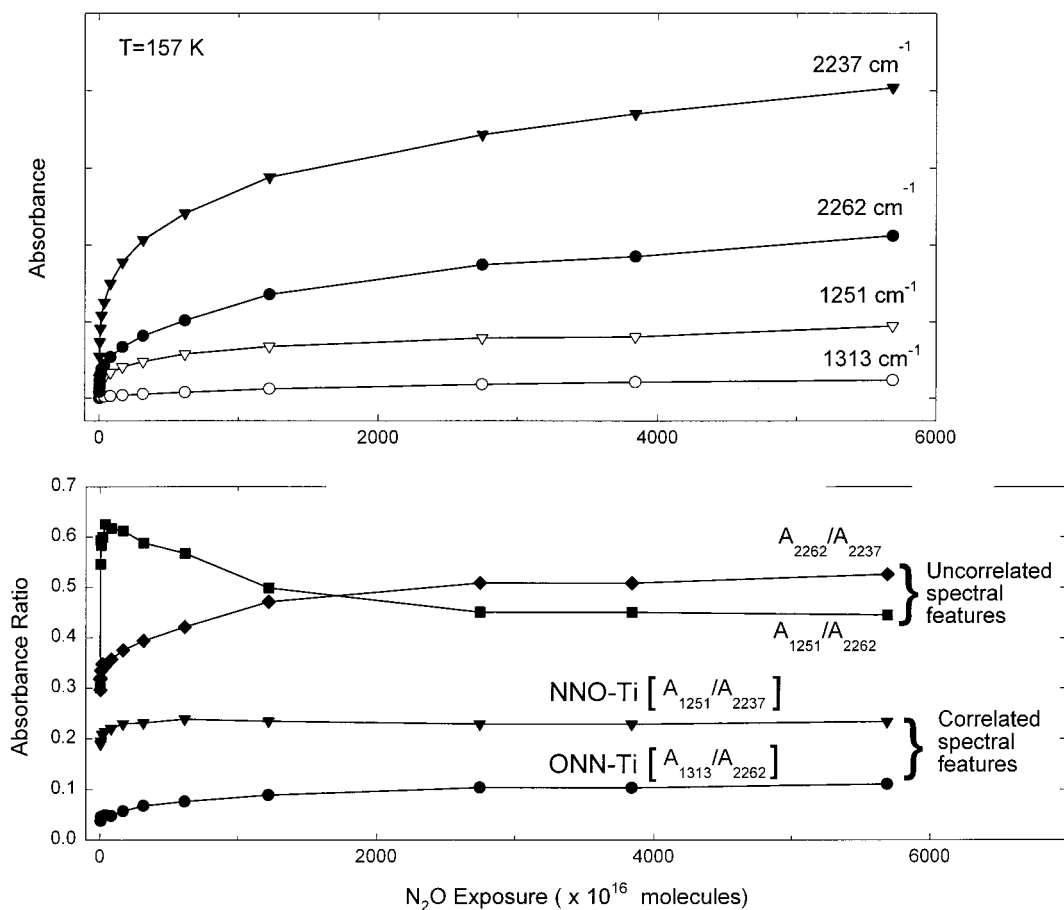


Figure 3. Development of the net absorbance for the major peaks as a function of increasing N_2O exposure is shown in the upper panel. The lower panel shows the ratio of the absorbance for different “pairs” of vibrational modes, emphasizing the correlated and the uncorrelated spectral features.

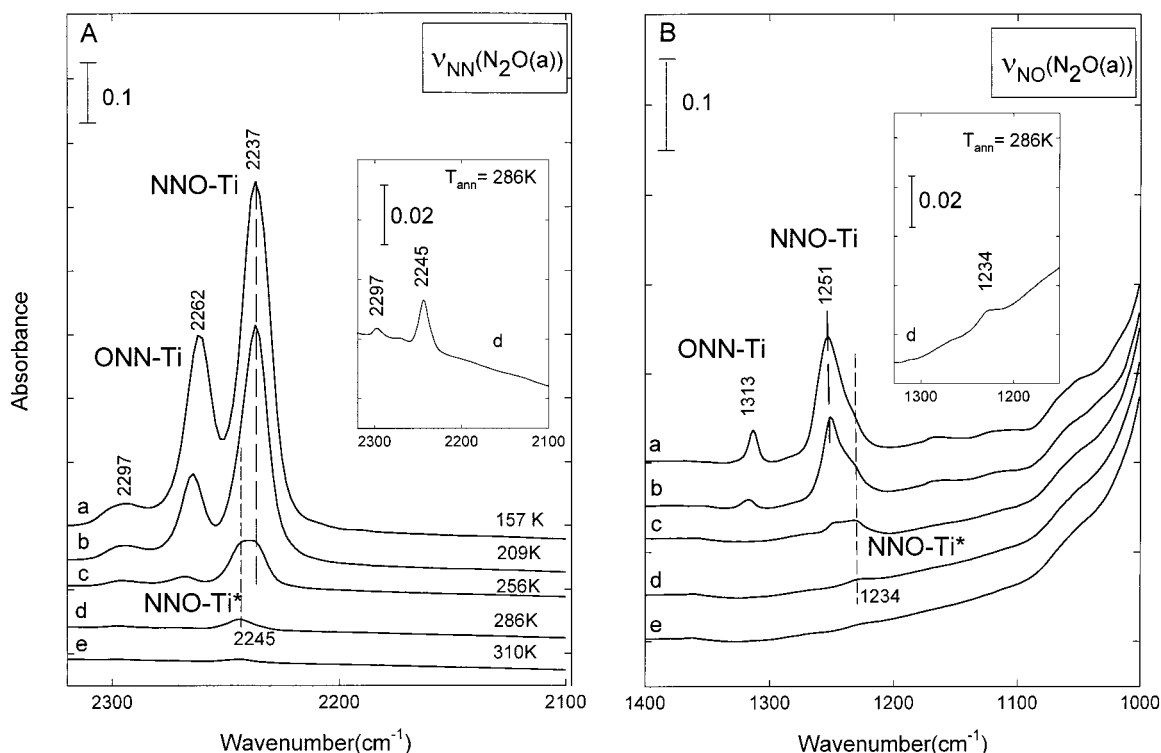


Figure 4. N₂O/TiO₂ thermal desorption process. IR spectra of the adsorbed N₂O molecules on TiO₂ powder are shown as a function of the temperature of the substrate: a, 157 K; b, 209 K; c, 256 K; d, 286 K; e, 310 K. The left panel corresponds to the nitrogen–nitrogen stretching vibration, and the right panel corresponds to the nitrogen–oxygen stretching vibration. The insets indicate the existence of a new O-bonded species characterized by the 2245/1234 cm^{−1} “pair” of vibrational modes.

relative rate of development was studied as the N₂O coverage was increased at 157 K. As shown in the lower panel of Figure 3, the ratios between the measured absorbances at 1251 and 2237 cm^{−1}, and that between the absorbances at 1313 and 2262 cm^{−1}, are almost constant for the entire range of N₂O exposures, indicating that these band pairs originate from the same surface bonding structures for N₂O(ads). Deviation from this constant value, seen at very small exposures, is due to the inherent error introduced when peaks of very small absorbance are evaluated. In contrast, the ratios between the absorbances of other peaks at 2262 and 2237 cm^{−1} and at 1251 and 2262 cm^{−1}, respectively, do not exhibit the same correlation. The detailed assignment of these vibrational modes is presented in the Discussion section. Briefly: (1) The correlated spectral features at 1251 and 2237 cm^{−1} are assigned to the N₂O molecule bound through O to the TiO₂ surface, and (2) the correlated spectral features at 1313 and 2262 cm^{−1} are assigned to the N₂O molecule bound through N to the TiO₂ surface.

2. Thermal Desorption Process for N₂O Adsorbed on TiO₂. Figure 4 shows, through IR spectral analysis, the thermal behavior of N₂O adsorbed on the TiO₂ sample. As the temperature increases, mainly N₂O desorption takes place. Interestingly, after the sample is annealed at 286 K (seen in the insets of Figure 4), the only absorption bands seen in the N–N stretch region are at 2245 and 2297 cm^{−1} and at 1234 cm^{−1} in the N–O stretch region. This suggests that the pair of absorption bands at 2245 and 1234 cm^{−1} are related to the same adsorbed species.

As seen in Figure 4, almost no molecular N₂O remains after the surface is heated to above 310 K and no detectable amount of adsorbed molecular nitrogen appears.

3. Photochemistry of N₂O Adsorbed on TiO₂. 3.1. Photochemistry at High N₂O Coverage. Figure 5 shows the IR spectra of a sample of TiO₂ containing N₂O at high coverage,

after different UV irradiation time periods. The temperature of the TiO₂ sample was constantly maintained at 157 K by electrical control. As the irradiation time increases, the intensity of all the N₂O modes decreases. No other additional peaks are formed during the irradiation process. The kinetics of the N₂O photodepletion for high N₂O initial coverages on TiO₂ are presented in Figure 6. The 2237 and 1251 cm^{−1} vibrational modes undergo a decay process with a similar kinetic constant. Also, the decrease in the absorbance of the 2262 cm^{−1} vibrational mode follows kinetics similar to those observed for the absorbance decrease in the 1313 cm^{−1} vibrational mode within the limit of error of measuring the absorbance of the small 1313 cm^{−1} band. Therefore, the photodepletion of the adsorbed N₂O molecules in time exhibits slightly different kinetic constants for the O-bound N₂O molecules compared to the N-bound molecules.

3.2. Photochemistry at Low N₂O Coverage. The photochemical depletion of N₂O adsorbed at smaller coverages on TiO₂ is shown in Figure 7. During the photodesorption process, the intensity of the 2237 cm^{−1} absorption band remains almost constant. In the region of the spectrum characteristic of the NO stretching mode of the adsorbed N₂O on TiO₂, the 1251 cm^{−1} absorption band also remains almost constant in intensity, but it shifts slightly toward a lower wavenumber as a new absorption band located at 1234 cm^{−1} starts to develop. Opposite to this behavior, the 2262 cm^{−1} absorption band decreases, and simultaneously, an increase in the intensity of the 2297 cm^{−1} absorption band is seen.

The development of the 2345 cm^{−1} adsorption band is attributed to adsorbed molecular N₂ produced by photochemical decomposition of N₂O. To determine whether the new absorption band is due to N₂ adsorbed on TiO₂, an experiment was carried out exposing TiO₂ at 157 K to N₂. The development of an absorption band was seen at 2345 cm^{−1}. This result is also

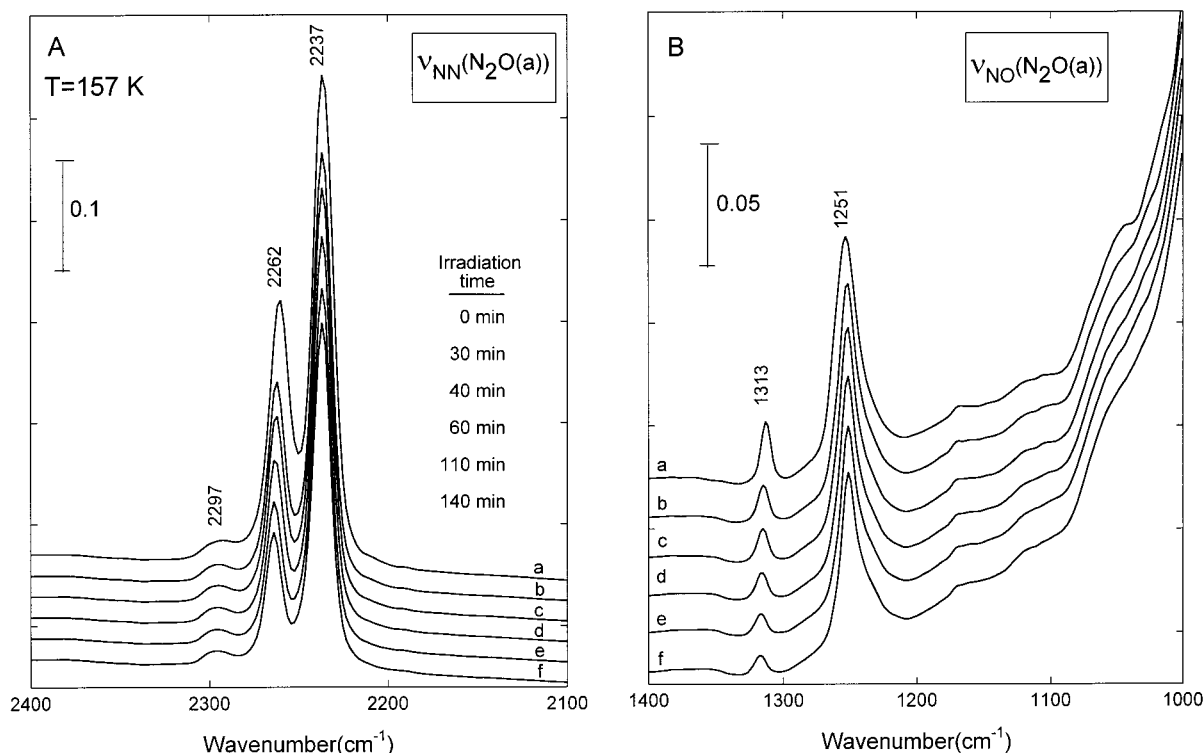


Figure 5. Photochemical depletion of N_2O at high initial coverage. IR spectra of the surface species formed during N_2O photochemistry on TiO_2 powder at 157 K are shown. The number of N_2O molecules added to the TiO_2 cell prior to irradiation was 6.0×10^{19} N_2O molecules. IR spectra are shown for the specified irradiation time periods: a, 0 min; b, 30 min; c, 40 min; d, 60 min; e, 110 min; f, 140 min.

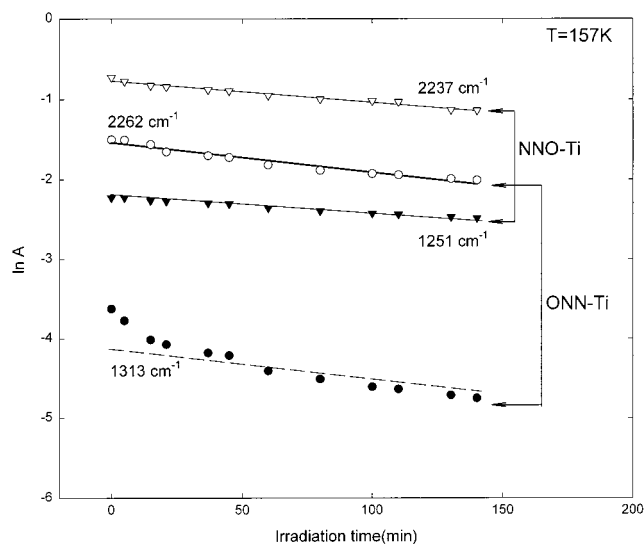


Figure 6. Kinetics plot of the photochemical depletion of N_2O adsorbed on the TiO_2 surface at high initial coverage. The number of N_2O molecules added to the TiO_2 cell prior to irradiation was 6.0×10^{19} N_2O molecules. The N-bonded species photodeplete faster than the O-bonded species. The dashed line has the slope of the fitted line for the 2262 cm^{-1} mode.

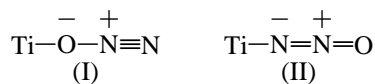
in agreement with the spectroscopic frequency of adsorbed N_2 on TiO_2 as reported in the literature.²⁹

NO was not a product in the photochemistry of the N_2O on TiO_2 powder for any of the coverages used. Figure 8 (upper panel) shows the typical IR spectrum of NO adsorbed on TiO_2 . Strong absorption bands develop at 1734 , 1869 , and 1898 cm^{-1} . A detailed discussion about NO adsorption on TiO_2 is found in ref 23. The lower panel of Figure 8 shows that, for the same spectral range, no adsorption bands were seen during N_2O irradiation. So, we can conclude that NO was not formed in the photochemistry of N_2O adsorbed on TiO_2 powder.

4. Control Irradiation Experiment. The photochemistry of N_2O adsorbed on TiO_2 was studied with the full Hg arc (2.1 – 5.0 eV). To exclude any artifact that would be caused by heating or other effects beyond our control through electrical maintenance of constant sample temperature during irradiation, a similar experiment was done with just visible light. The temperature of the TiO_2 sample was kept constant during this experiment at 157 K. As seen in Figure 9, no decrease in the spectral absorbance was seen and nitrogen was not produced during the visible light photoirradiation experiments. In contrast, a slight increase in the absorbance of all the N_2O vibrational modes was seen. This is attributed to the adsorption of N_2O molecules on the cold TiO_2 sample as they desorb from the walls of the cell as a consequence of long exposure to the photon source.

IV. Discussion

1. N_2O Bonding to TiO_2 . N_2O can bound through the nitrogen or oxygen end of the molecule to the TiO_2 surface. This is possible since, in accordance with the resonance structures, both terminal atoms of the molecule have a considerable amount of electron density. As shown in the Introduction, nitrous oxide adsorption has been studied on different surfaces. In these studies there is evidence for both N- and O-bonded complex formation:



The evidence for this double type of bonding was explained in an early study by Zecchina et al.¹³ They showed the presence of both N- and O-bonded N_2O surface species to Cr^{3+} on the surface of $\alpha\text{-Cr}_2\text{O}_3$. They assigned the modes at 2238 and 1237 cm^{-1} to an O-bonded adsorption complex on $\alpha\text{-Cr}_2\text{O}_3$ and the

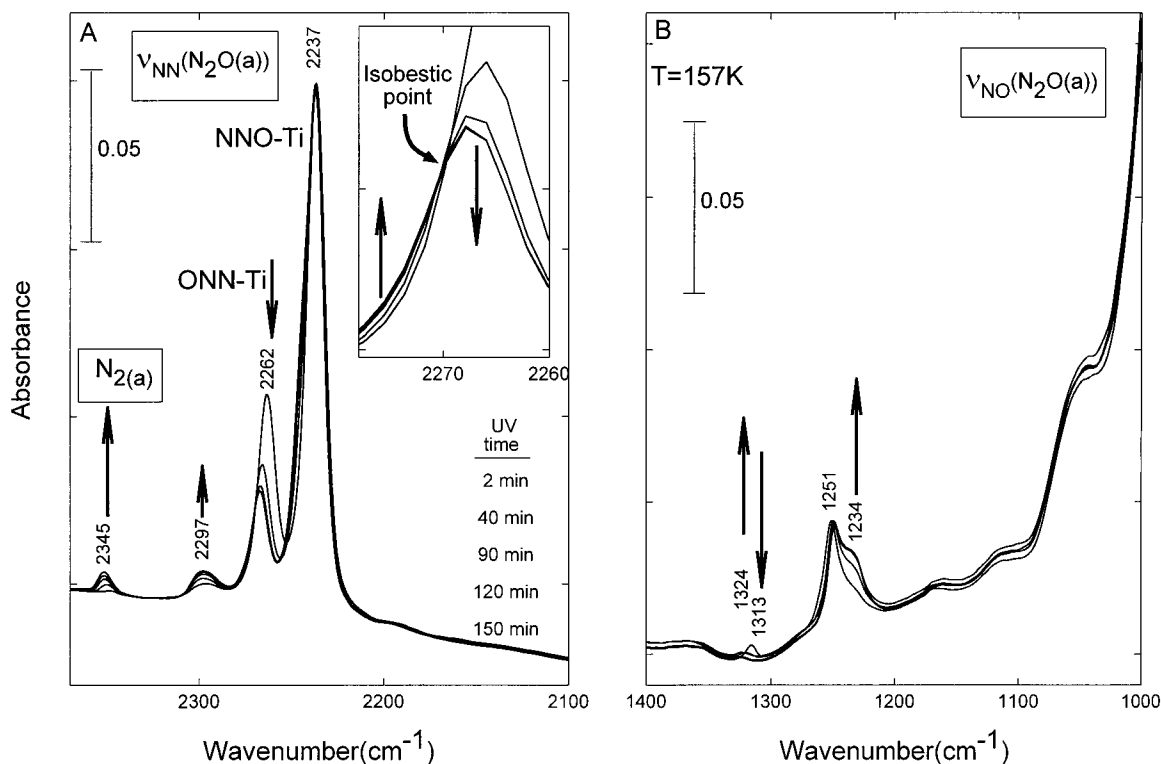


Figure 7. Photochemical depletion of N₂O at low initial coverage. IR spectra of the surface species formed during N₂O photochemistry on TiO₂ powder at 157 K are shown. The number of N₂O molecules added to the cell prior to irradiation was 1.20×10^{18} N₂O molecules. The left panel corresponds to the nitrogen–nitrogen stretching vibration, and the right panel corresponds to the nitrogen–oxygen stretching vibration.

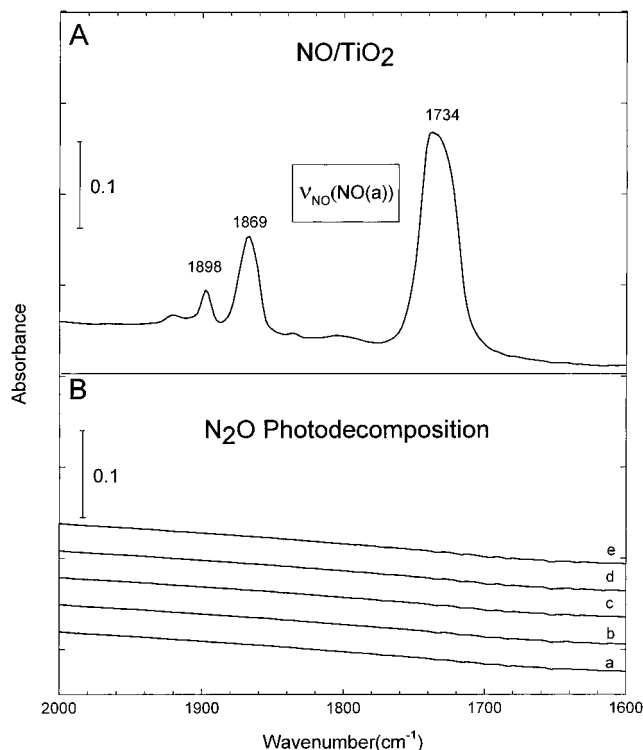


Figure 8. Lack of NO photoproduction from N₂O/TiO₂. The upper panel (A) shows the IR spectrum of the surface species formed when NO is adsorbed on the TiO₂ powder. The lower panel (B) shows the lack of NO production during irradiation of the N₂O adsorbed on the TiO₂ surface. The irradiation times are shown in Figure 7.

modes at 2305 and 1339 cm⁻¹ to an N-bonded adsorption complex on α -Cr₂O₃. Bonding through the oxygen atom should stabilize resonance structure I, which will result in a decrease in the N–O force constant and an increase in the N–N force

constant. As a consequence, comparing with the vibrational modes of the N₂O(g), a blue shift for the NN stretch (ν_{NN}) and a red shift for the NO stretch (ν_{NO}) of the adsorbed molecule should be seen for the O-bonded species. Therefore, the “pairs” of absorption bands, 2237/1251 cm⁻¹ and 2245/1234 cm⁻¹, are characteristic of the O-bonded molecules to the surface on two different sites. The 2245/1234 cm⁻¹ pair is observed upon N₂O thermal desorption (Figure 4) and is associated with a new type of Ti site designated Ti*.

In contrast, bonding through the N-end of the molecule should result in the stabilization of resonance structure II. The bonding in structure II could be compared to the isostructural and isoelectronic CO₂ molecule. The frequencies of the asymmetric and symmetric stretch for gas-phase CO₂ are at 2349 cm⁻¹ (IR-active) and 1388 cm⁻¹ (Raman-active). Therefore, it is expected that for the N-bonded species the characteristic vibrational modes will be situated in almost the same range as for CO₂ and the absorption peak associated with the symmetrical stretch will have a smaller absorbance in comparison with the asymmetric stretch. The weak intensity of the 1313 cm⁻¹ band confirms the assignment. In addition, the O-bonding increases the asymmetry of the molecule, while the N-bonding decreases it. On the basis of this assignment, the pair (2262/1313 cm⁻¹) is associated with the N-bonded species (II).

The fourth species seen is characterized by an absorption band located at 2297 cm⁻¹. The absorption band characteristic of the NO stretch mode (ν_1), which should accompany the NN absorption band (ν_3), is not seen in the low-frequency region of the spectrum. This may be due to the fact that the intensity of the 2297 cm⁻¹ mode is small. Since the 2297 cm⁻¹ band differs from the spectroscopically dominant N-bound and O-bound species, we assign it to a minority site on the surface, designated Ti*.

Therefore, we conclude that N₂O is adsorbed molecularly at 157 K on reduced TiO₂, forming basically four different

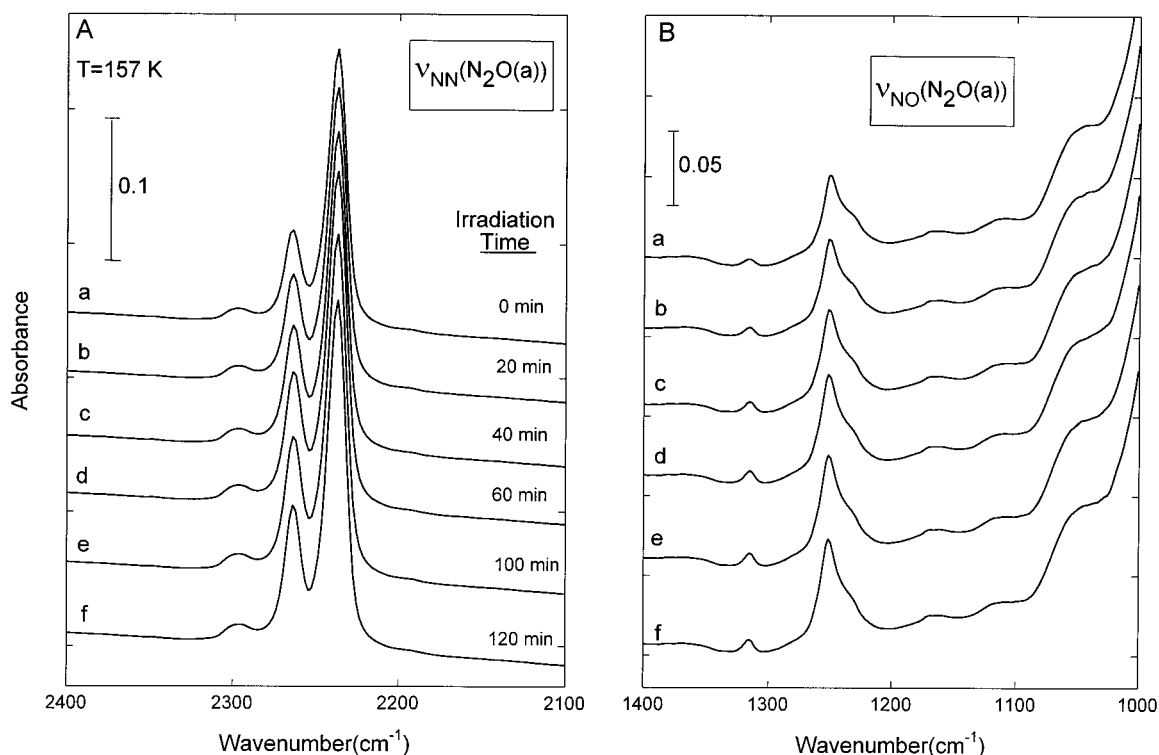


Figure 9. IR spectra of the surface species evolution during a control experiment with visible radiation ($\lambda > 400$ nm) instead of UV radiation. A lack of the photodepletion of N_2O adsorbed on TiO_2 powder at 157 K was seen during the vis irradiation experiment.

TABLE 1: Observed IR Absorption Bands for N_2O Adsorbed on TiO_2 and Their Assignment^a

	wavenumber (cm^{-1})		type of N_2O adsorbed species
	ν_3 (NN)	ν_1 (NO)	
N_2O (gas)	2224/2224 ¹⁵	1285/1285 ¹⁵	
N_2O adsorbed on TiO_2	2237/2238 ⁷	1251/1252 ⁷	NNO-Ti, O-bonded
	2245 ^b /2250 ⁷	1234 ^b /1235 ⁷	NNO-Ti*, O-bonded
	2262/2267 ⁷	1313/1310 ⁷	ONN-Ti, N-bonded
	2297/2290 ⁷	1324 ^c /1322 ⁷	ONN-Ti*, N-bonded

^a Our experimental data are compared with those from the literature.^{7,15} ^b These modes become visible only upon thermal desorption of the majority of the N_2O . ^c This mode becomes visible only upon photoactivation (see Figure 7).

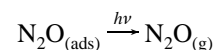
adsorption species. Two of these are on dominant Ti sites as Ti-ONN and Ti-NNO. Two are on minority Ti^* sites as Ti^* -ONN and Ti^* -NNO. The assignments of the absorption bands, based on the discussion made previously, are shown in Table 1. The formation of four adsorption species when N_2O was adsorbed on TiO_2 was also found by Ramis et al.,⁷ and their results were also included in Table 1.

2. N_2O Photochemistry. Defect sites in the titanium dioxide may be produced by annealing in a vacuum. This process removes O^{2-} anions, leaving behind anion vacancy defect sites, which are formally associated with Ti^{3+} ion centers. It has been shown that the Ti^{3+} centers are directly responsible for the chemical and photochemical reactivity of titanium dioxide.^{30–32}

It is believed that photon-induced electron–hole pair excitation within the near surface region of the TiO_2 is responsible for the electronic excitation of adsorbed molecules.³⁰ A photon excitation threshold energy near the band gap energy, $E_{\text{gap}} = 3.2$ eV, is required both for the photodesorption of molecules³⁴ and for surface photochemical reactions.^{35,36}

In these experiments we found that at high initial coverage only N_2O desorption is observed (Figure 5). At low coverage, N_2O undergoes a photochemically induced species interconversion process as well as producing adsorbed N_2 (Figure 7).

3.1. Photochemistry of N_2O Adsorbed at High Initial Coverages. For large coverages of N_2O adsorbed on TiO_2 , the only reaction observed is the desorption of the N_2O molecule, as seen in Figure 5:



The photochemical depletion, at 157 K, of the two types of bonded species formed as a consequence of N_2O adsorption on TiO_2 follow slightly different kinetics. As can be seen from the slopes of the decay of the IR absorbances in Figure 6, the N-bonded species deplete slightly faster than the O-bonded species.

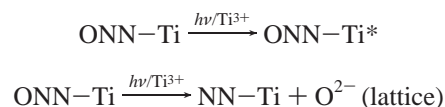
From Figure 5, we find that nitrogen was *not* a product of the N_2O photochemistry at high initial coverages on TiO_2 . The spectra of Figure 8 indicate that NO is also *not* a product of N_2O photolysis at any of the N_2O initial coverages on TiO_2 .

3.2. Photochemistry of N_2O Adsorbed at Low Initial Coverages. When N_2O is adsorbed on TiO_2 at smaller coverages, a major difference in the photochemical behavior is seen. Two main photochemical processes are observed: first, the formation of nitrogen, and second, the conversion of one type of adsorbed N_2O species into another type of species. The N-bonded species characterized by the absorption bands 2262/1313 cm^{-1} are converted to another N-bonded species characterized by absorption bands at 2297 and 1324 cm^{-1} . Taking into consideration that at least two different types of active centers³² are available on the titanium dioxide surface, this result suggests that, at lower N_2O coverages, conversion of N_2O from Ti-bonded species to Ti^* -bonded species occurs upon photochemical activation.

Upon comparing the photoreactivity of the different types of adsorbed species on titanium dioxide, it is obvious that they are different. The N-bonded species are depleted slightly faster than the O-bonded species. The intensity of the 2237 cm^{-1} absorption band that characterizes the O-bonded species at 157

K is almost not modified during the photochemical depletion of the adsorbed N₂O. Therefore, we can conclude that the O-bonded species are significantly more stable during UV irradiation regardless of the availability of the active sites.

So we can conclude that for small coverages of N₂O adsorbed on titanium dioxide the main processes are



Here Ti* is a Ti site that differs from the primary Ti site.

Therefore, as a consequence of the photochemistry of the adsorbed N₂O, the titanium dioxide surface will oxidize. It is well-known that N₂O can also act as an oxidant without photochemical activation and can reoxidize the reduced surface of titanium dioxide even at room temperature.¹⁸ Therefore, under photoradiation, N₂O can participate in the reoxidation of the surface, producing N₂ by its own decomposition.

V. Conclusions

- (1) N₂O adsorbs molecularly on TiO₂.
- (2) N₂O adsorption on the TiO₂ surface takes place through both the N and O end of the N₂O molecule.
- (3) UV photochemistry of N₂O adsorbed on TiO₂ is dependent on the N₂O coverage.
- (4) At high coverages of N₂O adsorbed on TiO₂, the photodesorption of N₂O takes place. No NO or N₂ was seen.
- (5) At low coverages of N₂O adsorbed on TiO₂, N₂O is photodepleted, producing adsorbed N₂.
- (6) The formation of NO as product of the photodepletion of N₂O adsorbed on TiO₂ was not seen for any of the N₂O initial coverages.

Acknowledgment. We thank the Army Research Office for support of this work.

References and Notes

- (1) Kapteijn, F.; Rodriguez-Mirasol, J.; Moulijn, J. A. *Appl. Catal. B: Environ.* **1996**, *9*, 25.
- (2) Kozirovski, Y.; Folman, M. *Trans. Faraday Soc.* **1969**, *65*, 244.

- (3) Hussain, G.; Rahman, M. M.; Sheppard, N. *Spectrochim. Acta* **1991**, *47A*, 1525.
- (4) Morterra, C.; Boccuzzi, F.; Coluccia, S.; Ghiotti, G. *J. Catal.* **1980**, *65*, 231.
- (5) Miller, T. M.; Grassian, V. H. *J. Am. Chem. Soc.* **1995**, *117*, 10969.
- (6) Miller, T. M.; Grassian, V. H. *Catal. Lett.* **1997**, *46*, 213.
- (7) Ramis, G.; Busca, G.; Bregani, F. *Gazz. Chim. Ital.* **1992**, *122*, 79.
- (8) Kim, Y.; Schreifels, J. A.; White, J. M. *Surf. Sci.* **1982**, *114*, 349.
- (9) Li, Y. X.; Bowker, M. *Surf. Sci.* **1996**, *348*, 67.
- (10) Kudo, A.; Nagayoshi, H. *Catal. Lett.* **1998**, *52*, 109.
- (11) Shultz, A. N.; Hetherington, W. M.; Baer, D. R.; Wang, L.-Q.; Engelhard, M. H. *Surf. Sci.* **1997**, *392*, 1.
- (12) Kubo, T.; Ems, T.; Atli, A.; Aruga, T.; Takagi, N.; Nishijima, M. *Surf. Sci.* **1997**, *382*, 214.
- (13) Zecchina, A.; Cerruti, L.; Borello, E. *J. Catal.* **1972**, *25*, 55.
- (14) Borello, E.; Cerruti, L.; Ghiotti, G.; Guglielminotti, E. *Inorg. Chim. Acta* **1972**, *6*, 45.
- (15) Herzberg, G. *Infrared and Raman Spectra*; Van Nostrand Reinhold Company: New York, 1945; p 278.
- (16) Yamada, H.; Person, W. B. *J. Chem. Phys.* **1964**, *41*, 2478.
- (17) Tanaka, K.; Blyholder, G. *J. Phys. Chem.* **1971**, *75*, 1037.
- (18) Cunningham, J.; Penny, A. L. *J. Phys. Chem.* **1974**, *78*, 870.
- (19) Cunningham, J.; Kelly, J.; Penny, A. L. *J. Phys. Chem.* **1971**, *75*, 617.
- (20) Anpo, M.; Aikawa, N.; Kubokawa, Y.; Che, M.; Louis, C.; Giamello, E. *J. Phys. Chem.* **1985**, *89*, 5017.
- (21) Anpo, M.; Aikawa, N.; Kubokawa, Y.; Che, M.; Louis, C.; Giamello, E. *J. Phys. Chem.* **1985**, *89*, 5689.
- (22) Anpo, M. *Surface Photochemistry*; Wiley Series in Photoscience and Photoengineering; Wiley: New York, 1996; Vol. 1.
- (23) Rusu, C. N.; Yates, J. T., Jr. *J. Phys. Chem. B* **2000**, *104*, 1729.
- (24) Basu, P.; Ballinger, T. H.; Yates, J. T., Jr. *Rev. Sci. Instrum.* **1988**, *59*, 1321.
- (25) Muha, R. J.; Gates, S. M.; Basu, P.; Yates, J. T., Jr. *Rev. Sci. Instrum.* **1985**, *56*, 613.
- (26) Spoto, G.; Morterra, C.; Marchese, L.; Orto, L.; Zecchina, A. *Vacuum* **1990**, *41*, 37.
- (27) Bickley, R. I.; Gonzales-Carreno, T.; Lees, J. S.; Palmisano, L.; Tilley, R. J. D. *J. Solid State Chem.* **1991**, *92*, 178.
- (28) Wong, J. C. S.; Linsebigler, A.; Lu, G.; Fan, J.; Yates, J. T., Jr. *J. Phys. Chem.* **1995**, *99*, 335.
- (29) Sakata, Y.; Kinoshita, N.; Domen, K.; Onishi, T. *J. Chem. Soc., Faraday Trans. 1*, **1987**, *83*, 2765.
- (30) Linsebigler, A.; Lu, G.; Yates, J. T., Jr. *Chem. Rev.* **1995**, *95*, 735.
- (31) Lu, G.; Linsebigler, A.; Yates, J. T., Jr. *J. Phys. Chem.* **1994**, *98*, 11733.
- (32) Rusu, C. N.; Yates, J. T., Jr. *Langmuir* **1997**, *13*, 4311.
- (33) Ballinger, T. H.; Wong, J. C. S.; Yates, J. T., Jr. *Langmuir* **1992**, *8*, 1676.
- (34) Lu, G.; Linsebigler, A.; Yates, J. T., Jr. *J. Chem. Phys.* **1995**, *102*, 3005.
- (35) Lu, G.; Linsebigler, A.; Yates, J. T., Jr. *J. Chem. Phys.* **1995**, *102*, 4657.
- (36) Linsebigler, A.; Lu, G.; Yates, J. T., Jr. *J. Chem. Phys.* **1995**, *103*, 9438.